Environmental Science and Pollution Research (2018) 25:14544–14550
https://doi.org/10.1007/s11356-018-1686-y

RESEARCH ARTICLE

The toxicity of cadmium ion (Cd^{2+}) to phycocyanin: an in vitro spectroscopic study

Zhenxing Chi[1,2] · Songwen Tan[1] · Xu Tan[3] · Lin Zhong[1] · Weiguo Li[1]

Received: 30 October 2017 / Accepted: 4 March 2018 / Published online: 11 March 2018

Abstract

The pollution of heavy metals is a severer problem for the ecosystems in waters. The toxicity of Cd^{2+} on phycocyanin (PC) is studied in molecular level in this work. The fluorescence quenching of PC is observed by the adding Cd^{2+} from 0 to 500 × 10^{-7} mol L^{-1}. From the theoretical calculation and the time-resolved fluorescence decay profiles, the fluorescence quenching of PC by Cd^{2+} is found to be static. The synchronous fluorescence spectra are used to study the change in amino acid residues of PC molecules, indicating that the effect of Cd^{2+} on the Trp of PC is more significant than the Tyr. The UV-Vis absorbance of tetrapyrrole decreases from 0.26 to 0.23 cps with increasing Cd^{2+} concentration, suggesting that Cd^{2+} affects the light adsorption and the photosynthesis function of PC. The circular dichroism spectra reveal that adding Cd^{2+} also changes the secondary structure (α-helix) of PC.

Keywords Cd^{2+} · Phycocyanin · Toxicity · Fluorescence characteristics · Molecule structure

Introduction

The water pollution of heavy metals has been a severer problem worldwide. In the eastern Beibu Bay of South China Sea, the contaminations of Zn, Cr, Pb, Cd, Cu, Hg and As were observed (Dou et al. 2013). In the southwestern South Atlantic Ocean, toxic heavy metals including Cd, As, Ag and Au were found in animal tissues (Cáceres-Saez et al. 2013). In the Red Sea, the contaminations of Cu, Zn, Pb, Cd, Fe and Mn were found in fish (El-Moselhy et al. 2014). Also, heavy metals with certain concentrations were found in rivers (Squadrone et al. 2013) and lakes (Li et al. 2013), resulting in a high risk of ecosystems in the waters.

Phycocyanin (PC), used for photosynthesis, is a very important protein in ecosystems, since many microorganisms in oceans, rivers and lakes are using PC for the conversion of solar energy to their chemical energy (French and Young 1952). The PC contains phycocyanobilin, which is a linear tetrapyrrole molecule with colour and fluorescence (Roda-Serrat et al. 2017). Since the heavy metal ions can easily bind with PC leading to fluorescence quenching, PC can be used as a biosensor for the detection of heavy metals (Hou et al. 2017; Mahato et al. 2012).

Cd^{2+} is a typical hazardous heavy metal in waters (Cardoso et al. 2013; Tang et al. 2017). The hazardous pollutants or high salinity can largely affect the bioactivity of organisms in the waters (Tan et al. 2017b; Tan and Li 2016). The Cd^{2+} with a concentration of 21 μg/mL has been reported to inhibit the growth (50%) of cyanobacteria (Dixit and Singh 2015). Evidence also shows that Cd^{2+} has higher toxicity than Pb^{2+}, Cu^{2+} and Cr^{3+} to the growth of cyanobacteria (Soeprobowati and Hariyati 2014). Another study of cyanobacteria has reported that the PC content decreases with increasing Cd^{2+} concentration. Forty-three percent inhibition of PC content was observed when the concentration of Cd^{2+} was 6 mg/L (Arunakumara and Zhang 2009). Yet no specific research has focused on the toxicity

Responsible editor: Philippe Garrigues

✉ Zhenxing Chi
zhenxingchi@hit.edu.cn

[1] Department of Environmental Engineering, Harbin Institute of Technology, Weihai, 2# Wenhua West Road, Weihai 264209, People's Republic of China

[2] Guangzhou Key Laboratory of Environmental Exposure and Health, School of Environment, Jinan University, Guangzhou 510632, People's Republic of China

[3] Department of Civil and Environmental Engineering, University of Technology Sydney, Sydney 2007, Australia

of Cd^{2+} to PC at molecular level experimentally. The influence of Cd^{2+} on fluorescence characteristics and protein structure of phycocyanin molecules has been studied in vitro in this work. The results show the binding of Cd^{2+} to PC biomolecules experimentally. This work provides the information for the related future works and may also benefit the understanding of the in vivo toxicity of Cd^{2+} to the marine organisms.

Materials and methods

Chemicals

The phycocyanin (PC) from *Spirulina platensis* was purchased from Binmei Biotech Co. Ltd., China. The PBS buffer with pH of 7.0 was prepared using $NaH_2PO_4 \cdot 2H_2O$ and $Na_2HPO_4 \cdot 12H_2O$ from Sinopharm Chemical Reagent Co. Ltd., China. $CdCl_2$ was purchased from Sigma-Aldrich, China. All chemicals were analytical reagent (AR) grade.

Fluorescence characteristics

Ten millimetres of PC samples were prepared by mixing the PBS buffer, PC and $CdCl_2$ solution for 15 min. The fluorescence spectra of the PC samples with Cd^{2+} concentrations of ($\times 10^{-7}$ mol L^{-1}) 0, 5, 10, 25, 50, 75, 100, 175, 250, 450 and 500 were measured at 298 and 308 K. The concentration of PC samples was 5.0×10^{-7} mol L^{-1} and the pH of solutions was 7.0. The samples were placed in the F4600 fluorescence spectrometer (Hitachi, Japan) for analysis. The excitation wavelength was set at 278 nm with emission wavelength range set at 280–530 nm. The slit width was 10 nm and the voltage was 400 V. The results were plotted using the Stern-Volmer equation ($F_0/F = 1 + K_{SV}[Q] = 1 + K_q\tau_0[Q]$) for dynamic quenching (Geethanjali et al. 2015) and modified Lineweaver-Burk equation ($\lg(F_0–F)/F = \lg K + n\lg[Q]$) for static quenching (Fu et al. 2016) to calculate the values of K_{SV}, K and n. In the equations, F_0 and F are the fluorescence intensities in the absence and presence of Cd^{2+}, K_{SV} is the quenching constant, K_q is the quenching rate constant, τ_0 is the lifetime of fluorophore ($\sim 10^{-8}$ s), Q is the concentration of Cd^{2+}, K is the binding constant and n is the number of binding

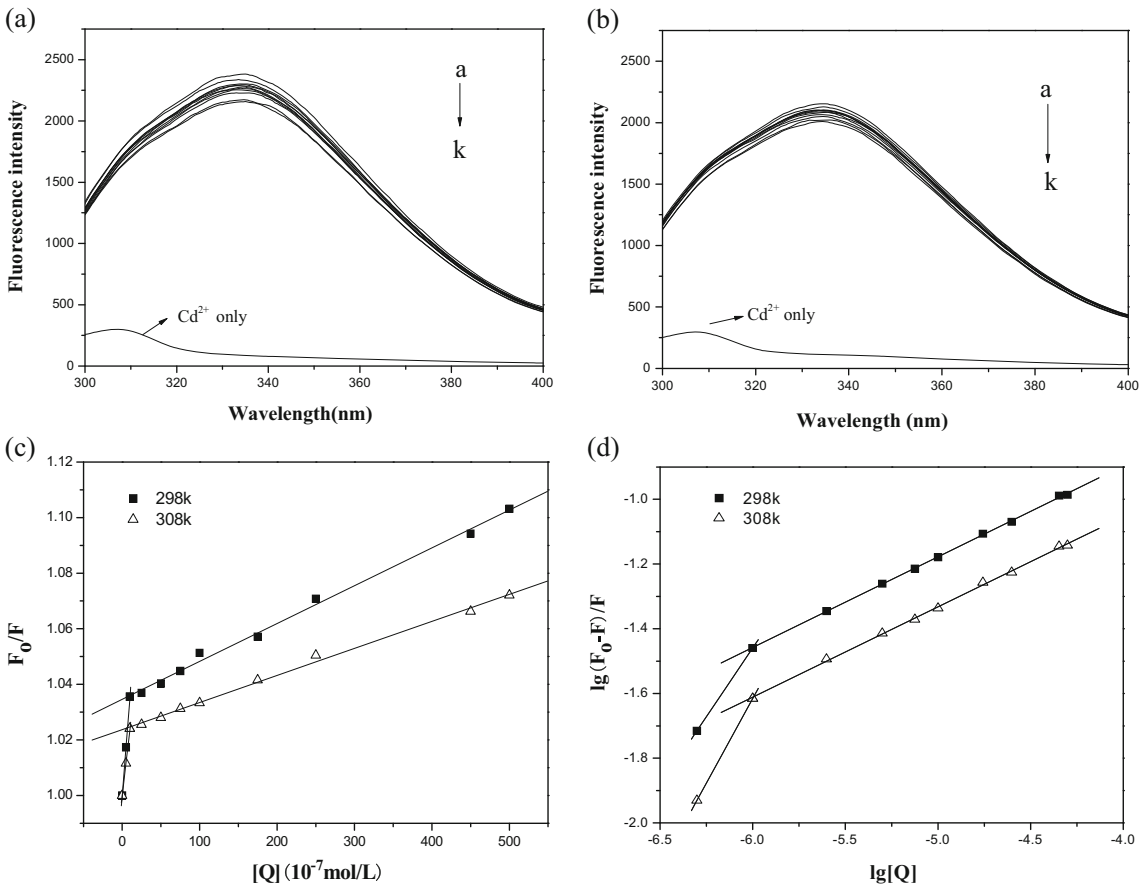

Fig. 1 Fluorescence spectra of the PC samples with Cd^{2+} concentrations of ($\times 10^{-7}$ mol L^{-1}) 0, 5, 10, 25, 50, 75, 100, 175, 250, 450 and 500 (from sub-a to sub-k) at 298 K (**a**) and 308 K (**b**). The Stern-Volmer plot (**c**) and the Lineweaver-Burk log-log plot (**d**) of fluorescence quenching by Cd^{2+} for PC samples at 298 and 308 K

Table 1 Results calculated from the Stern-Volmer equation with different Cd^{2+} concentration at 298 and 308 K

	T (K)	K_{sv} ($10^3 mol^{-1}$ L)	K_q ($10^{11} mol^{-1}$ s^{-1} L)	R
C (Cd^{2+}) ≤ 1×10^{-6} M	298	35.5	35.5	0.9999
	308	24.1	24.1	0.99982
C (Cd^{2+}) ≥ 1×10^{-6} M	298	1.36	1.36	0.99784
	308	0.97	0.97	0.99826

site. The time-resolved fluorescence decay profiles were measured for the PC samples with the Cd^{2+} concentrations of ($\times 10^{-7}$ mol L^{-1}) 0, 100 and 500 to further confirm whether the fluorescence quenching is dynamic or static (Gu et al. 2017).

The synchronous fluorescence spectra of PC samples with Cd^{2+} concentrations of ($\times 10^{-7}$ mol L^{-1}) 0, 5, 10, 25, 50, 75, 100, 175, 250, 450 and 500 were measured at $\Delta\lambda$ of 60 nm (for Trp emission spectra) or 15 nm (for Tyr emission spectra) (Bobone et al. 2014). The concentration of PC was 5.0×10^{-7} mol L^{-1}. The temperature was 298 K. The pH was 7.0. The excitation wavelength was set at 278 nm with emission wavelength range set at 265–325 nm. The slit width was 5 nm and the voltage was 400 V. The F_0/F values were plotted with the Cd^{2+} concentrations for the synchronous fluorescence spectra of PC samples at $\Delta\lambda$ of 60 or 15 nm.

The resonance light scattering spectra of water, Cd^{2+} solution, PC solution and PC-Cd^{2+} solution were measured at 298 K to identify if the solutes were well-mixed in solution (Pasternack and Collings 1995). The concentration of PC and Cd^{2+} were 5.0×10^{-7} and 5.0×10^{-6} mol L^{-1}, respectively. The pH was 7.0. The excitation wavelength was set at 228 nm with emission wavelength range set at 220–800 nm. The slit width was 2.5 nm and the voltage was 400 V.

Table 2 Results calculated from the modified Lineweaver-Burk equation with different Cd^{2+} concentration at 298 and 308 K

	T (K)	K (mol^{-1} L)	n	R
C (Cd^{2+}) ≤ 1×10^{-6} M	298	4357	0.85	1
	308	48,780	1.05	1
C (Cd^{2+}) ≥ 1×10^{-6} M	298	1.67	0.28	0.99977
	308	1.17	0.28	0.99947

Effect on the molecular structure of PC protein

Ten millimetres of PC samples were prepared by mixing the PBS buffer, PC and $CdCl_2$ solution for 15 min. The UV-Vis spectra of PC samples with the Cd^{2+} concentrations of ($\times 10^{-7}$ mol L^{-1}) 0, 5, 10, 25, 50, 75, 100, 175, 250, 450 and 500 were measured using the UV-Vis spectrophotometer (Shimadzu UV-2450, Japan). The temperature was 298 K. The concentration of PC samples was 5.0×10^{-7} mol L^{-1} and the pH of solutions was 7.0. The scan range was set at 190–800 nm to study the effect of Cd^{2+} on protein structure of PC, especially the tetrapyrrole (500–700 nm) for photosynthesis. The slit width was 1 nm. The circular dichroism (CD) spectra of PC samples with the Cd^{2+} concentrations of ($\times 10^{-7}$ mol L^{-1}) 0, 10, 25, 50, 100 were measured using the CD spectrometer (Jasco J-810, Japan). The scan range was set at 190–260 nm to study the change in α-helix structure (200–230 nm) (Chi et al. 2016) of the PC protein.

Results and discussion

Fluorescence quenching by Cd^{2+}

Fluorescence quenching has been used as a method to study the molecular interactions (Chi et al. 2017b, c). The fluorescence spectra of PC-Cd^{2+} samples are showed in Fig. 1a (at 298 K) and Fig. 1b (at 308 K) with different Cd^{2+} concentration. The

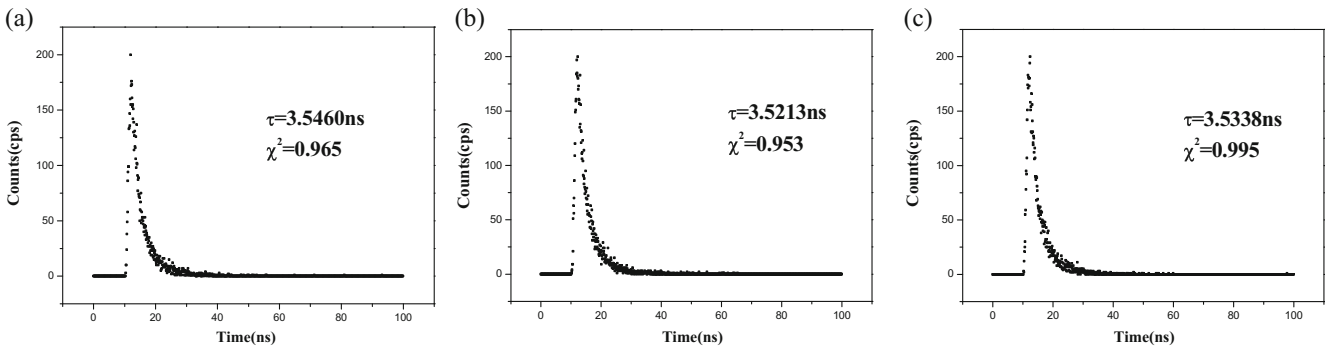

Fig. 2 Time-resolved fluorescence decay profiles of PC samples with the Cd^{2+} concentrations of ($\times 10^{-7}$ mol L^{-1}) 0 (**a**), 100 (**b**), 500 (**c**) at 298 K

Table 3 Thermodynamic parameters for the PC-Cd^{2+} interactions

	T (K)	ΔH (kJ mol^{-1})	ΔS (J mol^{-1} K^{-1})	ΔG (kJ mol^{-1})
C (Cd^{2+}) $\leq 1 \times 10^{-6}$ M	298	184.27	687.98	− 20.75
	308			− 27.63
C (Cd^{2+}) $\geq 1 \times 10^{-6}$ M	298	− 27.14	− 86.81	− 1.27
	308			− 0.40

peaks of the fluorescence spectra locate at 335 nm. The adding of Cd^{2+} from 0 to 500×10^{-7} mol L^{-1} does not shift these peaks but decrease the fluorescence intensity, showing the fluorescence quenching of PC by Cd^{2+}. At 298 K, the fluorescence intensity of PC decreased from about 2400 to 2150 ($\Delta = -250$), while at 308 K, the fluorescence intensity decreased from about 2150 to 2000 ($\Delta = -150$). Unlike dynamic quenching where the quencher and fluorophore collide, static quenching happens when the quencher binds with the fluorophore where high temperature limits the binding force and quenching degree (Gu et al. 2017). The Stern-Volmer plot (Fig. 1c) and the Lineweaver-Burk log-log plot (Fig. 1d) are generated based on the fluorescence spectra, and the calculated results are showed in Tables 1 and 2. The K_{sv} and K_q are smaller at high temperature (Table 1). When the concentration of Cd^{2+} is lower than 1×10^{-6} mol L^{-1}, the K_q values are 3.55×10^{12} mol^{-1} s^{-1} L at 298 K and 2.41×10^{12} mol^{-1} s^{-1} L at 308 K. When the concentration of Cd^{2+} is higher than 1×10^{-6} mol L^{-1}, the K_q values are 1.36×10^{11} mol^{-1} s^{-1} L at 298 K and 9.7×10^{10} mol^{-1} s^{-1} L at 308 K. However, these quenching rate constants are much larger than the maximum quenching rate constant which is 0.2×10^{11} mol^{-1} s^{-1} L for biomolecules (Rasoulzadeh et al. 2010), again showing that the Cd^{2+} quenching process is static. Calculated by the modified Lineweaver-Burk equation for static quenching (Table 2), the n values are 0.85 (at 298 K) and 1.05 (at 308 K) when the concentration of Cd^{2+} is lower than 1×10^{-6} mol L^{-1}, while the n values are 0.28 at 298 and 308 K when the concentration of

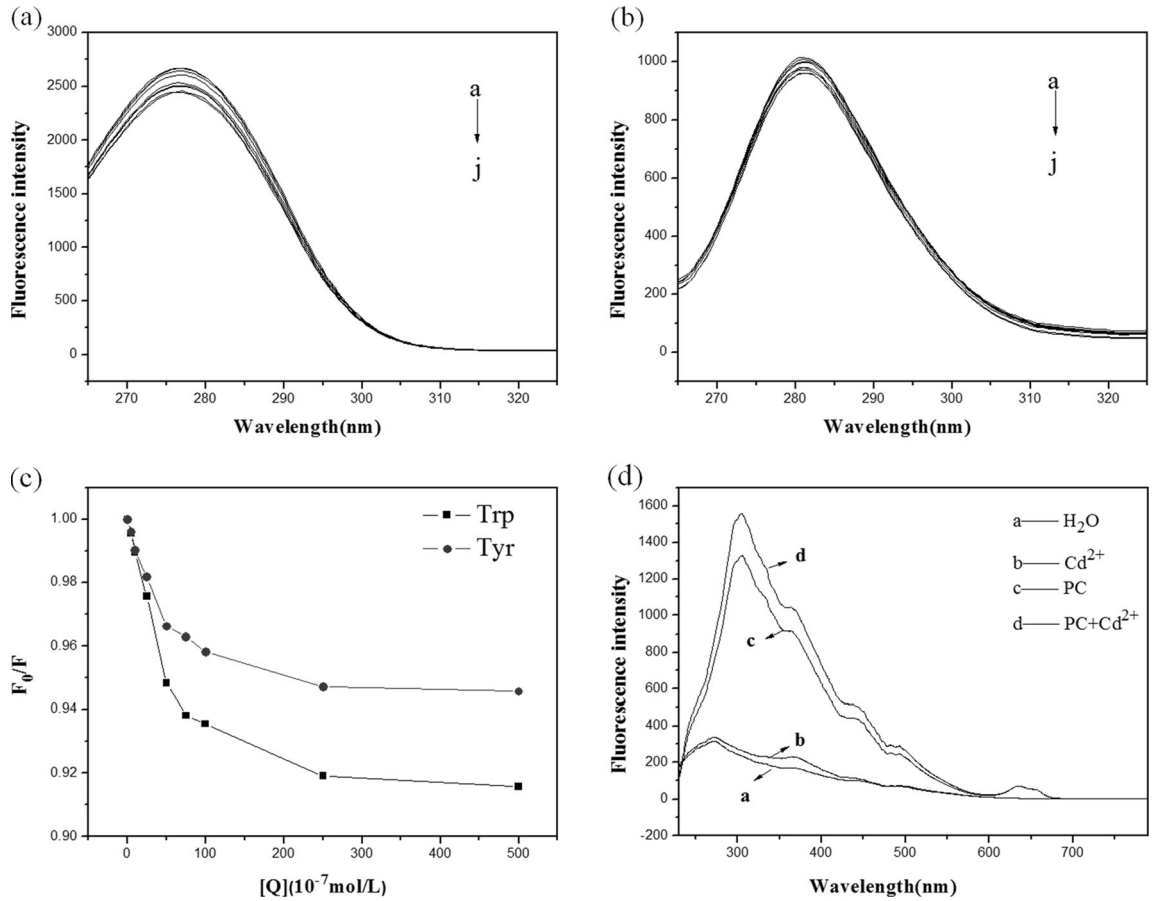

Fig. 3 Synchronous fluorescence spectra of PC samples with the Cd^{2+} concentrations of ($\times 10^{-7}$ mol L^{-1}) 0, 5, 10, 25, 50, 75, 100, 175, 250, 450 and 500 (from sub-a to sub-j) at $\Delta\lambda$ of 60 nm (**a**) or 15 nm (**b**); F_0/F plot for the synchronous fluorescence spectra of PC samples at $\Delta\lambda$ of 60 nm for Trp and 15 nm for Tyr (**c**). Resonance light scattering spectra of water, Cd^{2+} solution, PC solution and PC-Cd^{2+} solution (**d**)

Cd^{2+} is higher than 1×10^{-6} mol L^{-1}. For a static quenching process, the lifetime of excited fluorophore will not be significantly affected by the quencher (Chi et al. 2017a). Figure 2 shows the time-resolved fluorescence decay profiles of PC samples with different Cd^{2+} concentration. The lifetimes of PC samples were 3.55, 3.52 and 3.53 ns, respectively, when the Cd^{2+} concentrations were ($\times 10^{-7}$ mol L^{-1}) 0, 100 and 500. These values of the fluorescence lifetimes are similar, agreeing that the Cd^{2+} quenching process is static. The binding force of Cd^{2+} to PC is related with the thermodynamic parameters (Aki and Yamamoto 1989; Ross and Subramanian 1981). Table 3 listed the thermodynamic parameters for the PC-Cd^{2+} interactions with different Cd^{2+} concentration at 298 and 308 K. The negative ΔG values show that the quenching process is spontaneous. When the concentration of Cd^{2+} is lower than 1×10^{-6} mol L^{-1}, there is hydrophobic force between Cd^{2+} and PC molecules ($\Delta H > 0$, $\Delta S > 0$, $\Delta G < 0$) at 298 or 308 K. When the concentration of Cd^{2+} is higher than 1×10^{-6} mol L^{-1}, there are hydrogen bonding and VDW interactions between Cd^{2+} and PC molecules ($\Delta H < 0$, $\Delta S < 0$, $\Delta G < 0$). Therefore the K_q and n values are different under different Cd^{2+} concentration. Based on the force calculations, it is possible to model the molecular interactions via molecular docking in the future works (Tan et al. 2017a, c).

The synchronous fluorescence spectra are used to study the change in amino acid residues of PC molecules. Figure 3a shows the synchronous fluorescence spectra of PC samples for Trp emission spectra at $\Delta\lambda$ of 60 nm. With increasing the concentration of Cd^{2+}, the fluorescence intensity of PC largely decreases from 2700 to 2400 ($\Delta = -300$) with peaks at 278 nm. Figure 3b shows the synchronous fluorescence spectra of PC samples for Tyr emission spectra at $\Delta\lambda$ of 15 nm. With increasing the concentration of Cd^{2+}, the fluorescence intensity of PC decreases from 1000 to 950 ($\Delta = -50$) with peaks at 282 nm. The F_0/F values calculated from the synchronous fluorescence spectra were plotted in Fig. 3c. The F_0/F value for Trp residue decreases from 1.00 to 0.92 ($\Delta = -0.08$) with increasing Cd^{2+} concentration, while the F_0/F value for Tyr residue decreases from 1.00 to 0.95 ($\Delta = -0.05$), indicating that the effect of Cd^{2+} on the Trp residue of PC is more significant than the Tyr residue. Figure 3d shows the resonance light scattering spectra of water, Cd^{2+} solution, PC solution and PC-Cd^{2+} solution. The fluorescence intensity (~ 1600 cps) of PC-Cd^{2+} solution is similar to the sum of the fluorescence intensities of Cd^{2+} and PC, suggesting a good mixing of molecules in solution (Pasternack and Collings 1995).

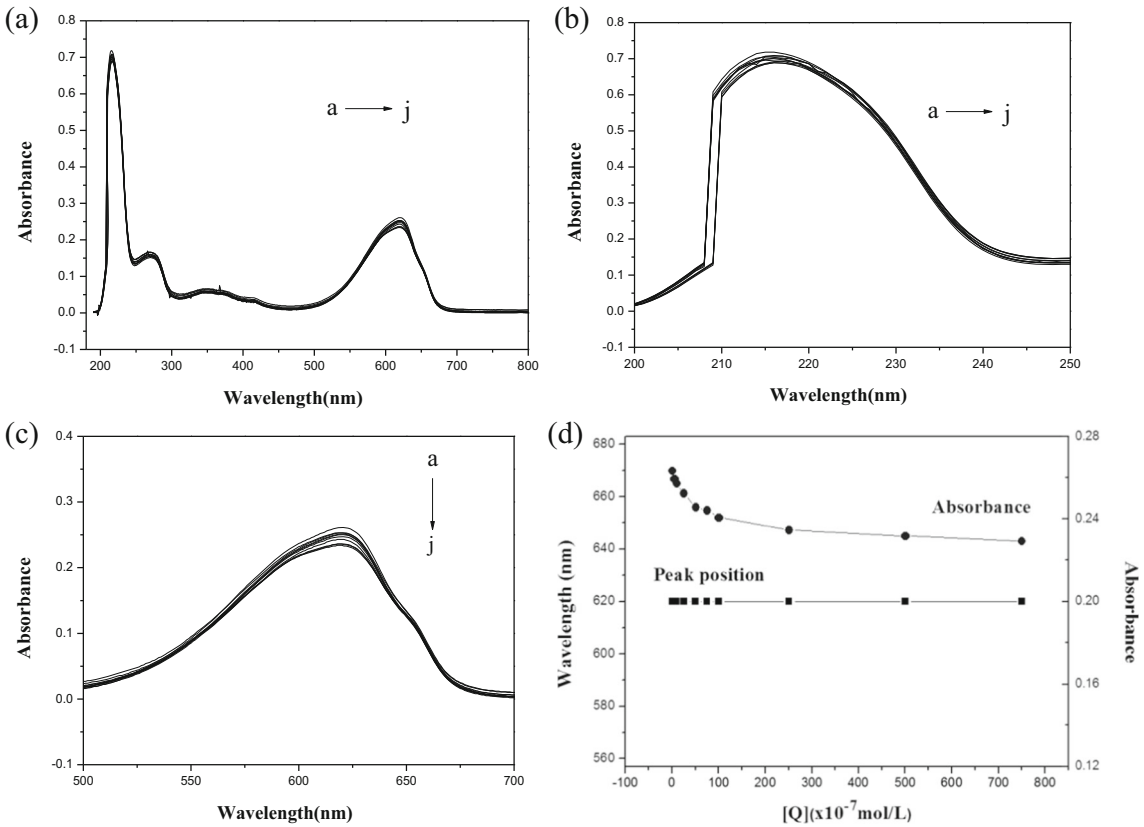

Fig. 4 UV-Vis spectra of PC samples with the Cd^{2+} concentrations of ($\times 10^{-7}$ mol L^{-1}) 0, 5, 10, 25, 50, 75, 100, 175, 250, 450 and 500 (from sub-a to sub-j) in the wavelength range of 190–800 nm (**a**), 200–250 nm (**b**) and 500–700 nm for tetrapyrrole (**c**). The changes in peak position and absorbance of tetrapyrrole with increasing the Cd^{2+} concentration (**d**)

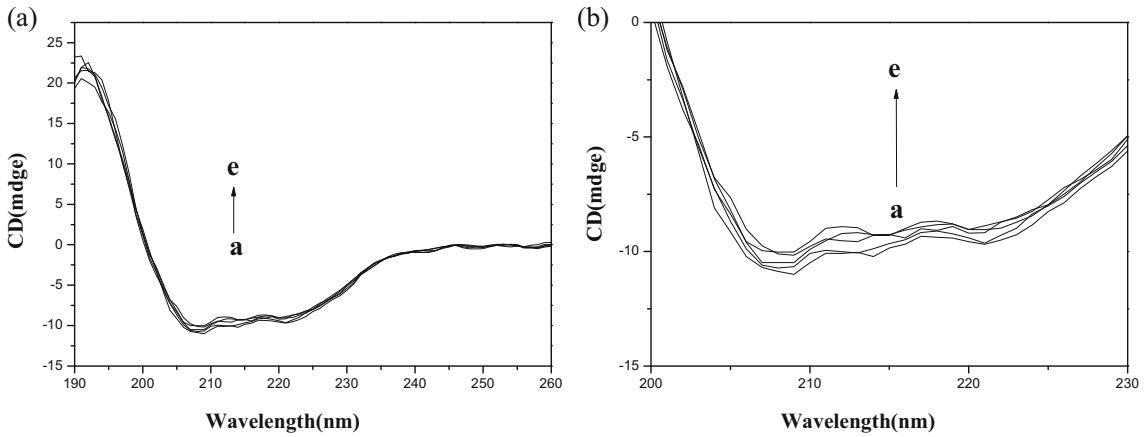

Fig. 5 Circular dichroism spectra of PC samples with the Cd^{2+} concentrations of ($\times 10^{-7}$ mol L^{-1}) 0, 10, 25, 50, 100 (from sub-a to sub-e) in the wavelength range of 190–260 nm (**a**) and 200–230 nm for α-helix structure of protein (**b**)

Change in the molecular structure of PC protein

Figure 4a shows the UV-Vis spectra of PC samples with the Cd^{2+} concentrations of ($\times 10^{-7}$ mol L^{-1}) 0, 5, 10, 25, 50, 75, 100, 175, 250, 450 and 500. The UV-Vis spectra of PC have four peaks, locating at 210 nm for protein skeleton, 270 nm for Phe residue, 350 nm for disulfide bond and 620 nm for tetrapyrrole. From the local large map (Fig. 4b), there is a slight decrease in the intensity for the peaks at about 210 nm, showing the effect of Cd^{2+} on the protein skeleton of PC. The detailed change in the protein structure is discussed in the next part with circular dichroism spectra. Figure 4c shows that the UV-Vis (light) absorbance of tetrapyrrole decreases from 0.26 to 0.23 cps (Fig. 4d) with increasing Cd^{2+} concentration. As the tetrapyrrole of PC contributes to photosynthesis, Cd^{2+} is suggested to affect the light adsorption and the photosynthesis function of PC.

Figures 5 shows the circular dichroism spectra of PC samples with the Cd^{2+} concentrations of ($\times 10^{-7}$ mol L^{-1}) 0, 10, 25, 50, 100 in the wavelength range of 190–260 nm (Fig. 5a) and 200–230 nm (Fig. 5b) for the α-helix structure of PC (Lu et al. 2007; Tan et al. 2018). The negative peaks of the α-helix structure locate at 208, 214 and 221 nm. With increasing the Cd^{2+} concentration, these negative peaks become smaller, showing a decrease of the α-helix structure. The change in the secondary structure of PC protein may due to interactions between Cd^{2+} with the amino acid residues of PC, leading to function loss of PC (Melo et al. 1997).

Conclusions

The effect of Cd^{2+} on phycocyanin (PC) was studied in this work. The fluorescence quenching of PC was observed by the adding Cd^{2+}. From the theoretical calculation and the time-resolved fluorescence decay profiles, the fluorescence quenching of PC by Cd^{2+} was found to be static that more fluorescence quenching was observed at relatively low temperature. The synchronous fluorescence spectra were used to study the change in amino acid residues of PC molecules, indicating that the effect of Cd^{2+} on the Trp of PC was more significant than the Tyr. The resonance light scattering spectra confirmed a good mixing of PC and Cd^{2+} in solution. The UV-Vis absorbance of tetrapyrrole decreased with increasing Cd^{2+} concentration, suggesting that Cd^{2+} affected the light adsorption and the photosynthesis function of PC. The circular dichroism spectra showed that adding Cd^{2+} changed the secondary structure (α-helix) of PC.

Funding information This work was supported by the National Natural Science Foundation of China (21707026), the Guangzhou Key Laboratory of Environmental Exposure and Health (No. GZKLEEH201613), and the Shandong Provincial Natural Science Foundation, China (ZR2014BQ033). The Natural Scientific Research Innovation Foundation in Harbin Institute of Technology (HIT.NSRIF.2014126) is also acknowledged.

Compliance with ethical standards

Conflict of interest The authors declare that they have no conflict of interest.

References

Aki H, Yamamoto M (1989) Thermodynamics of the binding of phenothiazines to human plasma, human serum albumin and α 1-acid glycoprotein: a calorimetric study. J Pharm Pharmacol 41:674–679

Arunakumara K, Zhang X (2009) Effects of heavy metals (Pb^{2+} and Cd^{2+}) on the ultrastructure, growth and pigment contents of the unicellular cyanobacterium Synechocystis sp. PCC 6803. Chin J Oceanol Limnol 27:383–388

Bobone S, van de Weert M, Stella L (2014) A reassessment of synchronous fluorescence in the separation of Trp and Tyr contributions in protein emission and in the determination of conformational changes. J Mol Struct 1077:68–76

Cáceres-Saez I, Guevara SR, Dellabianca NA, Goodall RNP, Cappozzo HL (2013) Heavy metals and essential elements in Commerson's

dolphins (*Cephalorhynchus c. commersonii*) from the southwestern South Atlantic Ocean. Environ Monit Assess 185:5375–5386

Cardoso SP, Lopes CB, Pereira E, Duarte AC, Silva CM (2013) Competitive removal of Cd^{2+} and Hg^{2+} ions from water using titanosilicate ETS-4: kinetic behaviour and selectivity. Water Air Soil Pollut 224:1535

Chi Z, Zhao J, You H, Wang M (2016) Study on the mechanism of interaction between phthalate acid esters and bovine hemoglobin. J Agr Food Chem 64:6035–6041

Chi Z, Li S, Wen Z, Shan Y (2017a) Mechanism of the toxicological interactions of decabrominated diphenyl ether with hemoglobin. Spectrosc Lett 50:1–6

Chi Z, Tan S, Li W, Wen Z, Song X, Wang M (2017b) In vitro cytotoxicity of decabrominated diphenyl ether (PBDE-209) to human red blood cells (hRBCs). Chemosphere 180:312–316

Chi Z, Zhao J, Li W, Araghi A, Tan S (2017c) In vitro assessment of phthalate acid esters-trypsin complex formation. Chemosphere 185: 29–35

Dixit S, Singh D (2015) Differential response of photosynthetic apparatus of cyanobacterium *Nostoc muscorum* to Pb and Cd toxicity. Photosynthetica 53:223–230

Dou Y, Li J, Zhao J, Hu B, Yang S (2013) Distribution, enrichment and source of heavy metals in surface sediments of the eastern Beibu Bay, South China Sea. Mar Pollut Bull 67:137–145

El-Moselhy KM, Othman A, El-Azem HA, El-Metwally M (2014) Bioaccumulation of heavy metals in some tissues of fish in the Red Sea, Egypt. Egypt J Basic Appl Sci 1:97–105

French CS, Young VK (1952) The fluorescence spectra of red algae and the transfer of energy from phycoerythrin to phycocyanin and chlorophyll. J Gen Physiol 35:873–890

Fu Z, Cui Y, Cui F, Zhang G (2016) Modeling techniques and fluorescence imaging investigation of the interactions of an anthraquinone derivative with HSA and ctDNA. Spectrochim Acta A Mol Biomol Spectrosc 153:572–579

Geethanjali H, Nagaraja D, Melavanki R, Kusanur R (2015) Fluorescence quenching of boronic acid derivatives by aniline in alcohols–a Negative deviation from Stern–Volmer equation. J Lumin 167:216–221

Gu W, Yan Y, Pei X, Zhang C, Ding C, Xian Y (2017) Fluorescent black phosphorus quantum dots as label-free sensing probes for evaluation of acetylcholinesterase activity. Sensors Actuators B Chem 250: 601–607

Hou Y, Yan M, Wang Q, Wang Y, Xu Y, Wang Y, Li H, Wang H (2017) C-phycocyanin from Spirulina maxima as a green fluorescent probe for the highly selective detection of mercury(II) in seafood. Food Anal Methods 10:1931–1939

Li F, Huang J, Zeng G, Yuan X, Li X, Liang J, Wang X, Tang X, Bai B (2013) Spatial risk assessment and sources identification of heavy metals in surface sediments from the Dongting Lake, Middle China. J Geochem Explor 132:75–83

Lu J-Q, Jin F, Sun T-Q, Zhou X-W (2007) Multi-spectroscopic study on interaction of bovine serum albumin with lomefloxacin–copper (II) complex. Int J Biol Macromol 40:299–304

Mahato P, Saha S, Suresh E, Di Liddo R, Parnigotto PP, Conconi MT, Kesharwani MK, Ganguly B, Das A (2012) Ratiometric detection of Cr^{3+} and Hg^{2+} by a naphthalimide-rhodamine based fluorescent probe. Inorg Chem 51:1769–1777

Melo EP, Aires-Barros M, Costa S, Cabral J (1997) Thermal unfolding of proteins at high pH range studied by UV absorbance. J Biochem Biophys Methods 34:45–59

Pasternack RF, Collings PJ (1995) Resonance light scattering: a new technique for studying chromophore aggregation. Science-New York Then Washington 269:935–939

Rasoulzadeh F, Asgari D, Naseri A, Rashidi MR (2010) Spectroscopic studies on the interaction between erlotinib hydrochloride and bovine serum albumin. DARU J Pharm Sci 18:179

Roda-Serrat MC, Christensen KV, El-Houri RB, Fretté X, Christensen LP (2017) Fast cleavage of phycocyanobilin from phycocyanin for use in food colouring. Food Chem 240(1):655–661

Ross PD, Subramanian S (1981) Thermodynamics of protein association reactions: forces contributing to stability. Biochemistry 20:3096–3102

Soeprobowati TR, Hariyati R (2014) Phycoremediation of Pb, Cd, Cu, and Cr by Spirulina platensis (Gomont) Geitler. Am J BioSci 2:165–170

Squadrone S, Prearo M, Brizio P, Gavinelli S, Pellegrino M, Scanzio T, Guarise S, Benedetto A, Abete M (2013) Heavy metals distribution in muscle, liver, kidney and gill of European catfish (Silurus glanis) from Italian Rivers. Chemosphere 90:358–365

Tan S, Li W (2016) Behaviour of fouling-related components in an enhanced membrane bioreactor using marine activated sludge. Bioresour Technol 220:401–406

Tan S, Chi Z, Shan Y, Wen Z, Li W (2017a) Interaction studies of polybrominated diphenyl ethers (PBDEs) with human serum albumin (HSA): molecular docking investigations. Environ Toxicol Pharmacol 54:34–39

Tan S, Cui C, Hou Y, Chen X, Xu A, Li W, You H (2017b) Cultivation of activated sludge using sea mud as seed to treat industrial phenolic wastewater with high salinity. Mar Pollut Bull 114:867–870

Tan S, Wang D, Chi Z, Li W, Shan Y (2017c) Study on the interaction between typical phthalic acid esters (PAEs) and human haemoglobin (hHb) by molecular docking. Environ Toxicol Pharmacol 53:206–211

Tan S, Tan X, Chi Z, Zhang D, Li W (2018) In vitro assessment of the toxicity of lead (Pb^{2+}) to phycocyanin. Chemosphere 192:171–177

Tang W, Zhang W, Zhao Y, Zhang H, Shan B (2017) Basin-scale comprehensive assessment of cadmium pollution, risk, and toxicity in riverine sediments of the Haihe Basin in north China. Ecol Indic 81: 295–301